JOURNAL OF COMPUTATIONAL PHYSICS 87, 488–493 (1990)

Note

TRIPIC: Triangular-Mesh Particle-in-Cell Code

I. Introduction

A particle-in-cell code using triangular meshes (TRIPIC code) is developed to simulate charged-particle motion in magnetostatic fields self-consistently. Triangular meshes are adequate to simulate in a computational region with curved boundaries. As an example, simulation results are presented for a light-ion beam (LIB) diode [1].

Up to now many particle simulations have been performed [2–8] to study a self-consistent interaction between charged particles and a field. In many codes usually rather regular space meshes are employed to describe the computational region. Recently we have a problem of, for example, a diode simulation for an intense particle beam. In this case the computational space region has nonuniform or curved boundaries.

In order to simulate such a problem, we developed the triangular mesh particle-in-cell code (TRIPIC) which employs triangular space meshes. The TRIPIC code is magnetostatic and 2.5-dimensional. In the TRIPIC code the relativistic equation of motion is solved and the interaction between particles and space meshes is accomplished by a simple method. A subroutine of a magnetostatic-field solver is based on a method developed by Winslow [9] and which is used in SUPERFISH [10] and TRIDIF [11] codes.

II. Code Structure

In the grid generator we use Winslow's method [9]. The coordinates at the boundaries of the computational model are set as the Dirichlet boundary conditions in the logical space. By using these conditions, the two Laplace equations are solved inversely by the successive over-relaxation (SOR) method in the logical-space meshes.

The relativistic equation of motion is solved by the Buneman scheme in the particle pusher:

$$dP/dt = q(E_p + v \times B_p). \tag{1}$$

Here P is the momentum, t the time, q the charge of the particle, E_p and B_p the electric and magnetic fields on the particle, v the velocity of the particle. A particle moves across the triangular meshes. To find the triangular mesh in which the par-

0021-9991/90 $3.00

Copyright © 1990 by Academic Press, Inc.
All rights of reproduction in any form reserved.

ticle is located, we perform the following computation: first, three triangles are composed of the particle position and any two vertixes of the mesh triangle. When the particle is inside this triangular mesh, the sum of the above three triangle areas is equal to the mesh area. If the width of the time step is small enough, the particle moves to a neighboring mesh of the old one. In addition, meshes are numbered in series. Therefore we can easily find a new position of the particle by searching a small number of the neighboring triangles, that is, at most 13 triangles. This is not time-consuming.

In the magnetostatic-field solver the following equations are used. These equations are solved by using the Coulomb gauge:

$$\text{div } D = \rho, \qquad \text{rot } B = \mu_0 J, \qquad D = \varepsilon_0 E, \tag{2}$$

where D is the elctric displacement, B the magnetic field, E the electric field, J the current density, ρ the electric charge density, μ_0 the magnetic permeability, and ε_0 the dielectric constant in the vacuum. We use Winslow's method for discretization. Figure 1 presents a part of the triangular (primary) meshes and the definition of the secondary mesh which is composed of a vertex and two midpoints of side of a primary mesh and whose area is one third of the primary one. Each vertex of a primary mesh is surrounded by six primary triangles. The control-volume method

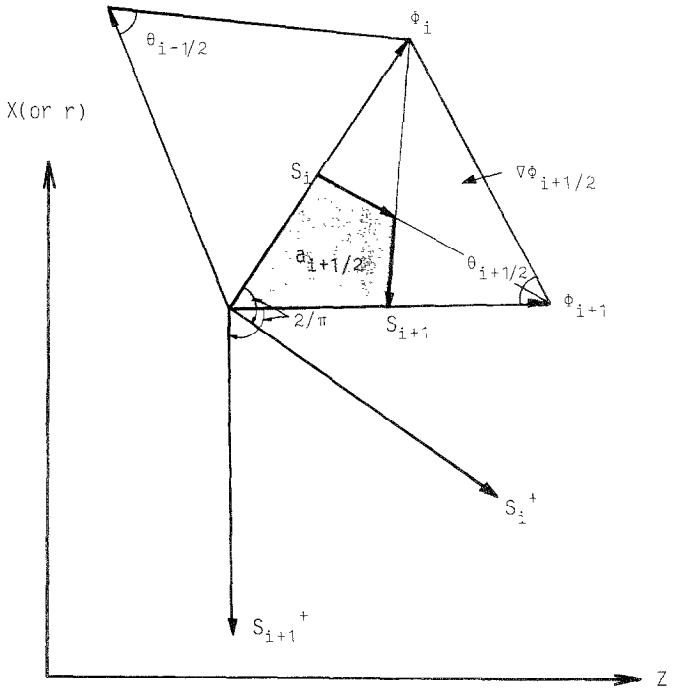

FIG. 1. The notations useful to the discretization of the field equations on the triangular mesh. The hatched region is the secondary mesh area.

is adapted to the dodecagon area consisted of six secondary meshes surrounding the vertex. Over the secondary mesh the generalized Poisson equation

$$\partial\Phi/\partial t = \nabla \cdot (\lambda \nabla \Phi) + s, \tag{3}$$

is integrated, assuming that the gradients of the physical quantities are constant in each triangular primary mesh, where Φ is the potential, t the time, λ the coefficient, and s the source term. Gauss' law is used for the first term on the right-hand side of Eq. (3). Finally we obtain the discretized form of the generalized Poisson equation on the triangular meshes:

$$\delta\Phi/\delta t = \left[\sum W_i(\Phi_i - \Phi) + G\right] \Big/ A, \tag{4}$$

$$W_i = (\lambda_{i+1/2} \cot \theta_{i+1/2} + \lambda_{i-1/2} \cot \theta_{i-1/2})/2,$$

$$A = \sum a_{i+1/2},$$

$$G = \sum a_{i+1/2} s_{i+1/2},$$

$$\sum = \sum_{i=1}^{6},$$

where W_i is the weight determined by the form of the primary meshes, $a_{i+1/2}$ the area of the secondary mesh. The first term at the right-hand side of Eq. (3) shows the sum of the fluxes. The angles of $\theta_{i+1/2}$ and $\theta_{i-1/2}$ are defined as shown in Fig. 1. In Fig. 1, S_i is the side vector combined between the center vertex and the vertex with the number i of the primary mesh, S_i^+ the vector rotated clockwise from S_i by the angle 90°.

The Dirichlet boundary condition is used for the static Poisson equation. For the magnetic-vector-potential equation the condition in which the perpendicular magnetic field becomes zero is imposed at the perfect conductor. In order to do so the magnetic vector potentials are resolved into the parallel and perpendicular components at the boundary surfaces. By using this decomposition, the coupled magnetic-vector-potential equations for the two components on the x (or r) $-z$ plane are solved. The direct Gauss forward-elimination and backward-substitution method is used in the matrix solver for the basic equations.

To accomplish the interaction between the particles and the space meshes, we use a simple weighting method. Each particle has a finite radius and meshes, locating in this circle, interact with the particle. The virtual radius of the particle is the maximum distance between the neighboring two grids. The field Ψ_p ($=E$ or B) on a particle is obtained by the following (see Fig. 2):

$$\Psi_p = \sum_{n=1}^{N} \frac{\Psi_n}{L_n} \Big/ \sum_{n=1}^{N} \frac{1}{L_n}. \tag{5}$$

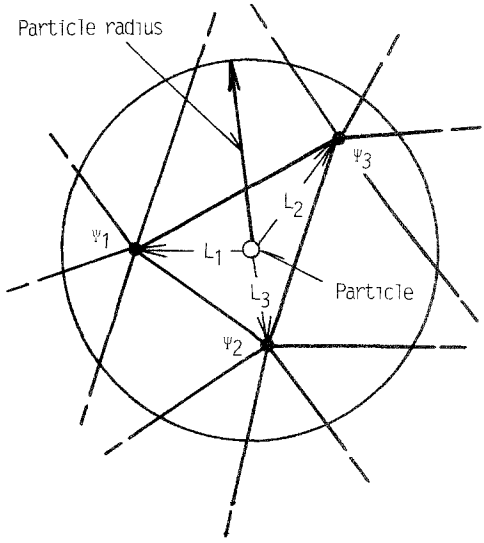

FIG. 2. The interaction of the particle and the meshes for the case of $N=3$. The particle has the finite radius. Ψ_n is the field (or the current or the charge densities) on the grid whose number is n, L_n the distance between the particle and the grid (number n) in the irregular triangular meshes.

Here Ψ_n is the field on the grid point in the circle of the particle, L_n is the length between the particle and the grid, n is the grid number, and N is the total number of the meshes interacting with the particle. In the weighting method, the weight is defined by the inverse of the distance between the particle and the mesh point. There is no difficulty in replacing $1/L_n$ with another weight function. Then the magnetostatic fields are obtained at the particle locations. The new current and charge densities are assigned to the grid from the particle by using this identical weight. We checked the conservation of physical quantities and found them well conserved.

In addition, the TRIPIC code has another subroutine for charged-particle generation. The particles are generated at the boundary surface to satisfy the space-charge limit condition. This optional subroutine is useful for simulating the electron and ion emission at the electrodes in an intense-LIB diode [1], for example.

III. EXAMPLE

In this section an example of the particle simulation is presented for a barrel type of the LIB diode. In this example the computational region is cylindrically and plane ($z=0$) symmetric. The applied voltage is 5MV and constant in time. There is no applied magnetic field inside the gap. The generated triangular meshes for the computation are shown in Fig. 3. The diode gap d_{a-k} is 0.8 cm, the height of the barrel $2 \cdot R1 = 12$ cm and the cathode radius $R_c = 6\sqrt{2}$ cm.

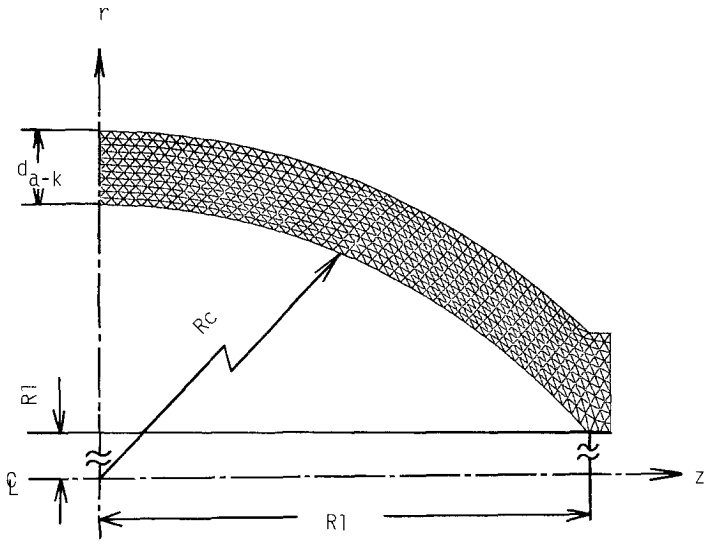

FIG. 3. The mesh structure, used in the simulation for a barrel type of a diode. The diode gap d_{a-k} is 0.8 cm, the height of the barrel $2 \cdot R1 = 12$ cm, the radius of the cathode $Rc = 6\sqrt{2}$ cm.

The computational results are shown in Fig. 4. The left-hand side of Fig. 4 shows the electron map and the right one is the proton map. In the curved region the behavior of the particles is simulated. Due to the self-magnetic field electrons preferentially drift to near the $z = 0$ plane.

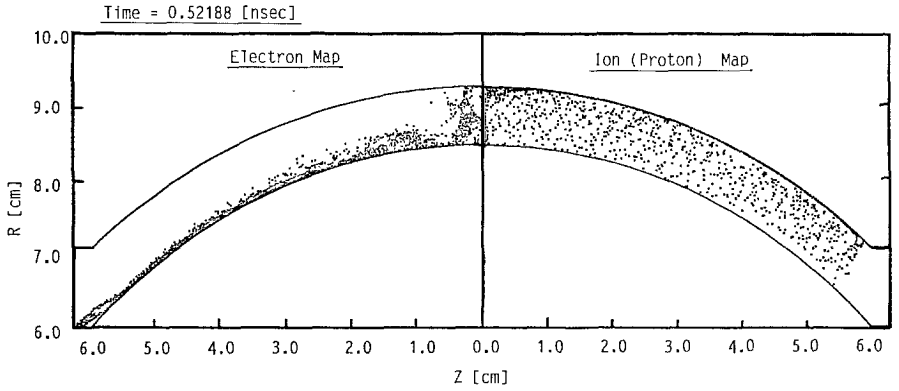

FIG. 4. The electron and proton maps in a barrel type of a diode. The applied voltage is 5 MV. The computation employs both cylindrical symmetry and symmetry about the $z = 0$ plane. The total mesh nmber employed is 574, the total super-particle numbers for ion and electron 1424 and 1747 at this snap shot respectively, and the time steps for electron and ion $\Delta t_e = 0.348$ ps $= (0.2\, L_{n\min}/c)$ and $21 \times \Delta t_e$, respectively, where $L_{n\min}$ is the minimum L_n and c the light speed. A sub-cycle is used in a particle pusher.

IV. SUMMARY

The triangular-mesh particle-in-cell (TRIPIC) code was developed to simulate the behavior of particles self-consistently in a curved region. The code has many applications. The example treated here for a diode with curved electrodes is a useful application.

ACKNOWLEDGMENTS

The study was partly supported by the Institute of Plasma Physics, Nagoya University, and the computer center of Tokyo University, Japan. The authors would like to extend their appreciation to Provessor W. G. Hoover, of the Department of Applied Science, University of California, Davis, for his help with English language.

REFERENCES

1. J. P. VANDEVENDER *et al.*, in *Proceedings, 6th Int. Conf. on High-Power Particle Beams, 1986*, p. 43.
2. J. M. DAWSON, *Rev. Mod. Phys.* **55**, 403 (1983).
3. C. K. BIRDSALL AND A. B. LANGDON, *Plasma Physics via Computer Simulation* (McGraw–Hill, New York, 1985).
4. R. W. HOCKNEY AND J. W. EASTWOOD, *Computer Simulation Using Particles* (McGraw–Hill, New York, 1981).
5. For example, T. TAJIMA AND J. M. DAWSON, *Phys. Rev. Lett.* **43**, 276 (1979).
6. For example, S. A. SLUTZ, D. B. SEIDEL, AND R. S. COATS, *J. Appl. Phys.* **61**, 11 (1987).
7. For example, A. B. LANGDON AND B. F. LASINSKI, *Methods Comput. Phys.* **16**, 327 (1976); D. W. HEWETT AND A. B. LANGDON, *J. Comput. Phys.* **72**, 121 (1987).
8. For example, B. GOPLEN, R. E. CLARK, AND S. J. FLINT, Mission Res. Corp. Report No. MRC/WDC-R-001, (1979) (unpublished); J. P. QUINTENZ, *J. Appl. Phys.* **49**, 4377 (1978); B. MARDER, *J. Comput. Phys.* **68**, 48 (1987).
9. A. M. WINSLOW, *J. Comput. Phys.* **2**, 149 (1967).
10. K. HALBACH AND R. F. HOLSINGER, *Part. Accel.* **7**, 213 (1976).
11. J. R. FREEMAN, *J. Comput. Phys.* **41**, 142 (1981).

RECEIVED: April 1, 1988; REVISED: April 28, 1989

MASAMI MATSUMOTO

Department of Electrical Engineering
Yonago National College of Technology
Yonago, Tottori 683, Japan

SHIGEO KAWATA

Department of Electrical Engineering
Faculty of Engineering, Nagaoka University of Technology
Nagaoka, Niigata 940-21, Japan